Revista Brasileira de Ciência do Solo

Division – Soil in Space and Time | Commission – Soil Genesis and Morphology

Identification of plinthite or saprolite residue in soils with high textural contrast in the southern Brazil

Mariana Rigueira da Costa Pereira[(1)], **Fabrício de Araújo Pedron**[(2)*], **Ricardo Simão Diniz Dalmolin**[(2)], **Ricardo Bergamo Schenato**[(2)] and **José Eduardo Dias Alves**[(3)]

[(1)] Universidade Federal de Santa Maria, Departamento de Solos, Programa de Pós-Graduação em Ciência do Solo, Santa Maria, Rio Grande do Sul, Brasil.
[(2)] Universidade Federal de Santa Maria, Departamento de Solos, Santa Maria, Rio Grande do Sul, Brasil.
[(3)] Universidade Federal de Santa Maria, Curso de Graduação em Agronomia, Santa Maria, Rio Grande do Sul, Brasil.

ABSTRACT: Soils classified as Alisols are very frequent in the sedimentary agricultural areas of southern Brazil. The presence of red mottles with morphology similar to plinthite and saprolite residue is very common in these soils, and its identification can be considered a difficult task, both in the field and in the laboratory. The incorrect identification of these redoximorphic features can affect soils' taxonomic and technical classification. We aimed to compare morphological, physical, chemical and mineralogical data to identify reddish mottles, possibly plinthites or saprolite residues, that occur in soils with high textural contrast in southern Brazil. Four soil profiles classified as *Argissolos Bruno-Acinzentados* (Alisols) were sampled. Matrix and mottles samples from the horizon Bt, CB, C and Cr were separated and subjected to morphological, granulometric, total sand fractionation, chemical extractions of iron and potassium and mineralogical features. Peds from each horizon were submitted to the submersion test in water for 2 and 8 hours and to 5 wetting and drying cycles. The mineralogy indicated the low degree of alteration of the samples, with abundant presence of 2:1 minerals and feldspars, even in the clay fraction. The saprolite resisted in the water submersion tests, making it difficult to interpret the results for the correct identification between plinthites and saprolite fragments. The morphological field data associated with the results of the tests of submersion in water, the cycle of wetting and drying, the dissolution of K and mineralogy, indicate the saprolithic nature of the mottles in all horizons and profiles. The submersion test in water for 2 and 8 hours was not efficient for the plinthite/saprolite identification. The cycle of wetting and drying tests allowed the identification of saprolite.

Keywords: redoximorphic features, mottles, plinthization, soil morphology.

*** Corresponding author:**
E-mail: fapedron@ufsm.br

Received: July 16, 2022
Approved: October 25, 2022

How to cite: Pereira MRC, Pedron FA, Dalmolin RSD, Schenato RB, Alves JED. Identification of plinthite or saprolite residue in soils with high textural contrast in the southern Brazil. Rev Bras Cienc Solo. 2022;46:e0220079. https://doi.org/10.36783/18069657rbcs20220079

Editors: José Miguel Reichert and Pablo Vidal Torrado.

INTRODUCTION

In the highland sedimentary environment of the Central Depression of Rio Grande do Sul State (RS), southern Brazil, soils with low permeability in the B horizon, called *Argissolos* (Acrisols, Alisols, Luvisols) and *Plintossolos* (Plinthosols), are very common, especially in the lower portion of the landscape, mainly due to the high textural contrast and the fluctuation of the water table level (Pedron et al., 2012; Almeida and Santos, 2021). The low permeability favors the formation of shallow (up to 1.00 m) and imperfectly drained profiles (solum), with the occurrence of redoximorphic features from the top of the Bt horizon to the Cr, providing adequate conditions for the formation of plinthites and petroplinthites (Pedron and Dalmolin, 2019).

The periodic excess of moisture in the subsurface soil horizons promotes the formation of depletion zones, where the reduction of iron oxides occurs, its mobilization out of the profile or concentration in zones with higher O_2 concentration (Eze et al., 2014). This process, mainly associated with desilication, eluviation/iluviation, ferrolysis and plinthization, results in mottles that are sometimes difficult to be appropriately identified in the field, generating confusion, especially between plinthites and saprolite residues (Almeida and Santos, 2021).

Saprolite can be defined as a layer that presents different degrees of alteration and maintains the rock structure, being able to be excavated by a spade (Pedron et al., 2009). Plinthite is a morphological feature consisting of a mixture of clay with quartz or other minerals, rich in iron or iron and aluminum and poor in organic carbon (Anjos et al., 2007). Under the action of repeated wetting and drying cycles, plinthite is irreversibly consolidated, becoming petroplinthite (Santos et al., 2018). Despite their different nature, plinthites and saprolite residues are morphologically similar in the Alisols studied because both occur as reddish mottles with polygonal (irregular) and reticulate (blocky) pattern spreaded into the horizon matrix.

The presence of plinthite or petroplinthite can alter the retention and movement of water (Daniels et al., 1978) and roots in the soil. In addition, they promote limitations to mechanization when close to the soil surface (Miguel et al., 2013; Pedron et al., 2015). In this way, their wrong identification results in a misunderstanding taxonomic and technical classification.

In an attempt to understand the boundary between soil and saprolite, Pedron et al. (2015) verified the presence of reddish mottles occurring in the B, CB, C and Cr horizons of *Argissolos Bruno-Acinzentados* (Alisols) in the Central Depression region of RS, Brazil. In the C and Cr horizons these mottles were identified based on their morphology as saprolite fragments, as they present rock structure; however, in the Bt horizons, the greater degree of alteration of the material made their identification difficult. Another aspect highlighted by the authors is the abundant presence of mica and K-feldspar in the rock (sediments of Sanga do Cabral Formation), which can support the mottles identification. Due to the lower weathering of the underlying horizons, it is expected that the potassium contents will increase in depth, suggesting the saprolithic nature of the mottles present in this portion of the soil.

During several field events, different experienced pedologists identified these features as plinthites, highlighting the difficult distinction regarding interpretation between plinthic and saprolithic materials. Daniels et al. (1978) already warned about this difficulty among field technicians in the USA. In Brazil, there is still little knowledge about saprolite among soil science professionals (Pedron et al., 2009; Juilleret et al., 2018).

In recent years, some studies have been dedicated to the theme, trying to qualify the understanding of plinthites in Brazilian soils. Jacomine et al. (2010) carried out tests to confirm the presence of plinthites in soil samples, based on wetting and drying cycles of

the samples and their resistance to crumbling and hardening, also used by Almeida and Santos (2021). The stability of plinthites after different drying methods was evaluated by Martins et al. (2018). All the studies reaffirm the interpretative difficulty of the data obtained, as well as the high variation of the results. None of them considered the comparison between plinthite and saprolite residue, an action that is still complex and without laboratory data that can support a field interpretation.

Some scientific questions still need answers: Can the tests of sample submersion in water and the wetting and drying cycles, widely used to confirm the presence of plinthites, manage to separate saprolite samples? Can the chemical dissolution of potassium and iron and mineralogical analysis help to differentiate plinthite from saprolite? This study aimed to compare morphological, physical, chemical and mineralogical data to identify reddish mottles in soils with high textural contrast in southern Brazil.

MATERIALS AND METHODS

Study area characterization

The study was conducted in the geomorphological province of the Central Depression, on the southern portion of the Paraná Basin, in the municipality of São Pedro do Sul, Rio Grande do Sul, Brazil. The sampling sites have a smooth undulating relief, with altitudes ranging from 112 to 149 m (Table 1). The local geology is constituted by sedimentary deposits in alluvial plains, of the Lower Triassic, coming from the Sanga do Cabral formation. The geologic material is composed of fine to very fine quartz-feldspathic sandstones. It also shows abundant presence of micas, carbonate concretions and intercalations with siltstone/claystone. This composition causes low permeability to the material (Sartori, 2009). The climate is classified as humid subtropical without a dry season (Cfa) according to Köppen, with average annual rainfall of 1708 mm and average annual temperatures of 19.2 °C (Maluf, 2000).

Four soil profiles were evaluated and identified as P1, P2, P3 and P4. Soils were classified according to the Brazilian Soil Classification System - SiBCS (Santos et al., 2018), as *Argissolos Bruno-Acinzentados Ta Alumínicos*, and in the FAO (Food and Agriculture Organization) international soil classification system, the World Reference Base for Soil Resources (WRB) (IUSS Working Group WRB, 2015) as Alisols (Table 1). For each profile, samples were collected from the Bt, CB, C and Cr horizons and RCr layer. The samples were submitted to manual separation of the mottles, air dried, manually ground and passed through 2 mm sieves.

Morphological analysis

The morphological description was performed in the field, according to the methodology recommended by Santos et al. (2015). The sequence of horizons, depth, wet color,

Table 1. Environmental data and taxonomic classification of soils with high textural contrast in southern Brazil

Profile[1]	Altitude	Geographic coordinates[1]	Land-use	Taxonomic classification[2]	
				SiBCS	WRB
	m				
P1	147	0758892/6718084	Natural grassland	PBACva abrúptico	AL-ap
P2	149	0758688/6718063	Natural grassland	PBACva abrúptico	AL-ap
P3	130	0757163/6717878	Natural grassland	PBACva típico	AL-ha
P4	112	0750767/6717385	Natural grassland	PBACva típico	ALha

[1] UTM projection fuse 21J, Datum WSG 84. [2] PBACva: *Argissolo Bruno-Acinzentado Ta alumínico* (SiBCS). AL-ap: Abruptic Alisol, AL-ha: Haplic Alisol (WRB).

consistency and textural class were recorded in the matrix and mottles samples of the selected horizons (Bt, CB, C and Cr). Size and volume (percentage scraped with a tile spade and percentage after cleaning with a knife) were also recorded for the mottles. The volume estimate was obtained by comparing the profile section with the percentage of coverage card available in Schoeneberger et al. (2012) and Santos et al. (2015).

To identify the presence of plinthites, two peds from each horizon were weighed, placed in 2 mm sieves and recipients with water, constituting one of the three repetitions per sample. The first test was the peds submersion in water for two hours (Wood and Perkings, 1976), in which the samples were submitted to gentle manual shaking for five times, repeated at 30 min intervals. The second test was the peds submersion in water for eight hours (Daniels et al., 1978), in which the samples were also submitted to gentle manual shaking for five times. The samples resistant to disaggregation in water were oven-dried at 50 °C and weighed. To verify the dispersion of data from the repetitions, the standard deviation of the mean was calculated for each sample.

In addition to the disaggregation tests in water, five cycles of wetting and drying were also performed according to Jacomine et al. (2010), over a period of approximately two months. Peds from each horizon were placed on plastic trays and exposed to the sun, followed by saturation with water. After that, the material was subjected to sun drying again. This process was repeated until the last cycle. After drying and saturated, the samples remained under these conditions for at least 24 h. The counting of the cycles started with the saturation of the samples after the air drying of the peds sampled in the field. In the laboratory, the samples were placed in a 2 mm sieve and saturated to observe the hardness and nature of the remaining material, which was transferred to aluminum cans, oven-dried and weighed.

The weathering degree of mottles was estimated using the weathering classes applied to sedimentary saprolites according to Pedron et al. (2010). The Bt and CB mottles of all profiles were classified in the class I5 (very weathered saprolite), the C and Cr mottles were class I4 (weathered saprolite) and the RCr layer was class I3 (moderate weathered rock).

Physical analysis

The granulometric composition was determined by the pipette method (Teixeira et al., 2017) in the air-dried fine earth (ADFE) of each horizon in samples previously separated in matrix and mottles, in addition to the rocks of the studied profiles. Sodium hydroxide 1 mol L^{-1} was used as a chemical dispersant, and the physical dispersion was carried out by 2 h shaking without the nylon spheres, as indicated by Gubiani et al. (2021), to avoid the fractionation of saprolithic material in the sand fraction. The sand fraction was separated by wet sieving, while the clay fraction was determined by sedimentation. The silt fraction was obtained by the difference between the sand and clay fractions in relation to the total mass of each sample.

The sand was sieved into five fractions: very coarse sand (2 - 1.00 mm), coarse sand (1.00 - 0.50 mm), medium sand (0.50 - 0.250 mm), fine sand (0.250 - 0.106 mm) and very fine sand (0.106 - 0.053 mm). The sieves were manually shaken and the fractions were weighed. The coarse fragments (>2 mm) were also reported for each horizon.

Chemical analysis

Iron (Fe) contents in the matrix and mottles samples of each horizon were determined by selective dissolutions with dithionite-citrate-bicarbonate – DCB (Mehra and Jackson, 1960), acid ammonium oxalate – AAO (McKeague and Day, 1966) and digestion with hydrochloric acid – HCl (Dick and Kämpf, 1988). For all the procedures mentioned, the iron contents were obtained by atomic absorption spectrophotometry.

Exchangeable potassium (K) was extracted with Mehlich-1 solution (HCl 0.05 mol L^{-1} + H_2SO_4 0.0125 mol L^{-1}) according to Jackson et al. (1986), while non-exchangeable K was obtained via digestion with HNO_3 1 mol L^{-1} (Knudsen et al., 1983) adapted by Martins et al. (2004). Potassium content was obtained by the flame photometry.

Mineralogical analysis

Clay fraction of the matrix and mottles samples was obtained by the centrifuge method (Jackson, 1985). The fractions obtained by centrifugation were saturated with K (KCl 1 mol L^{-1}) and Mg ($MgCl_2$ 1 mol L^{-1}) according to the recommendations of Karathanasis and Hajek (1982) and Whitting and Allardice (1986).

Clay minerals were analyzed on oriented slides. The clays were submitted to the following treatments: saturated with K and Mg and read at room temperature (K25 and Mg25); saturated with Mg and solvated with glycerol (Mg+glycerol) and saturated with K and then heated to 100, 300 and 550 °C (K100, K300 and K550). The rock and sand samples were ground and sieved (0.106 mm) and analyzed into powder.

The equipment used to perform the XRD analysis was a Shimadzu XRD 6100 X-ray diffractometer, composed of a copper anode (Cu Kα 0.154 nm) and a nickel filter (Ni), with a scan speed of 0.02 degrees 2θ s^{-1}, operating in the ranges from 3 to 30 °2θ for clay samples and from 3 to 65 °2θ for sand and rock samples, with acceleration voltage of 30 kV and current of 30 mA. The identification of mineral phases was determined according to Brindley and Brown (1980) and Resende et al. (2005).

RESULTS

Table 2 presents the morphological data of the matrix and the mottles of the evaluated horizons. For all profiles, the solum (horizons A+B) showed a depth of less than 1.00 m. The presence of the Cr horizon between 90 and 1.30 m stands out. In general, the matrix samples are greyish, with a hue of 10 YR, high values and low chromas, while the mottles present reddish colors, with hues varying between 5 YR and 10 R.

Wet consistency ranged from firm to friable at the Bt horizon of all profiles. In the matrix of the C and Cr horizons, there was a variation from firm to friable in P1 and P2 and from very firm to extremely firm in P3 and P4. The mottles showed a predominantly friable consistency in the C horizon, varying in Cr from firm to very firm in P1 and P2 and from friable to firm in P3 and P4.

The Bt horizons of P1 and P2 presented wet consistency very plastic to very sticky in the matrix and a predominance of plastic to sticky in the mottles. In the C horizon, a slightly plastic to slightly sticky consistency predominated in the matrix. The nonplastic to nonsticky condition was also verified in the mottles of P3 and P4, a pattern that also prevails in the Cr horizon.

The volume of mottles on the profile face cleaned with a knife (toilet) in the Bt horizons ranged from 2 to 5 %. In the C horizon, there were volumes of 5 to 15 %, reaching 40 % in P3 and P4 (only scraped face). In the Cr of P1, the mottles constituted 60 % of the horizon for the two situations evaluated, while in P3 there was a variation from 15 to 40 % for the profile with toilet and only scraped, respectively. This difference can be seen in figure 1. The diameter of the mottles increases in depth, ranging from 1 to 15 mm in the Bt horizons, from 5 to 50 mm in the C and reaching up to 200 mm on the Cr horizon of the P1.

Table 3 presents the data obtained using the morphological tests of submersion in water for 2 and 8 h and the cycles of wetting and drying to identify plinthites. The highest values in the first two tests occurred in P3 and P4, with higher percentages

Table 2. Morphological description of the matrix and mottle samples in soils with high textural contrast in southern Brazil

Samples	Layer	Moist color (Munsell)	Consistence*		Mottles		
			Moist	Wet	Toilet	Scraped	Ø medium
	m				%		mm
P1 Bt matrix	0.63-0.90	10 YR 4/4	fi	vp/vs	5	5	1-5
P1 Bt mottle		10 R 3/6	fr	p/s			
P1 C matrix	0.90-1.05	10 YR 5/4	fi-fr	p/s	15	15	5-30
P1 C mottle		10 R 3/6	fr	np/ss			
P1 Cr matrix	1.30-1.70+	10 YR 6/1	fi-fr	np/ns	60	60	30-200
P1 Cr mottle		2.5 YR 3.5/7	fi-mf	np/ns			
P2 Bt matrix	0.60-0.90	10 YR 4/3	fi-fr	vp/vs	2	2	2-5
P2 Bt mottle		2.5 YR 3/6	fr	p/s			
P2 CB matrix	0.87-1.05	10 YR 4/1	fi	sp/ss	5	35	10-50
P2 CB mottle		5 YR 4/6	fr	p/s			
P2 Cr matrix	1.30-1.50+	10 YR 5/1	fi	sp/ss	25	40	5-30
P2 Cr mottle		2.5 YR 2.5/4	fi-vf	p/s			
P3 Bt matrix	0.29-0.47	10 YR 5/3	fi-fr	sp/s	2-5	5	2-8
P3 Bt mottle		2.5 YR 4/8	fr	sp/ss			
P3 C matrix	0.66-0.90	10 YR 5/2	ef	sp/ss	10	40	2-5
P3 C mottle		5 YR 4.5/6	fr-fi	np/ns			
P3 Cr1 matrix	0.90-1.12	10 YR 6/2	ef	np/ns	15	40	10-100
P3 Cr1 mottle		5 YR 5/7	fr-fi	np/ns			
P4 Bt matrix	0.53-0.76	10 YR 6/3	fi	p/s	5	2	2-15
P4 Bt mottle		5 YR 4/6	fr	p/s			
P4 C matrix	0.76-1.24	10 YR 6/1.5	vf-ef	sp/ss	10	40	15-40
P4 C mottle		5 YR 4.5/7	fr	np/ns			
P4 Cr matrix	1.24-150+	10 YR 7/2	vf-ef	np/ns	10	30	15-40
P4 Cr mottle		5 YR 5/8	fr-fi	np/ns			

* Consistence: fr: friable; fi: firm; mf: very firm; ef: extremely firm; np: nonplastic; sp: slightly plastic; p: plastic; vp: very plastic; ns: nonsticky; ss: slightly sticky; s: sticky; vs: very sticky.

in the Bt horizons (83 and 82 %) and C (80 and 71 %) of P3 (Figure 2) and in the C horizons (74 and 70 %) and Cr (69 and 83 %) from P4 (Figure 3). The lowest values were observed in P1 and P3.

Not all samples increased material disaggregation when comparing the results of the 2 and 8 h tests. There was a predominance of low standard deviation in relation to the means obtained in the tests, with values of zero or very close to it. For the C and Cr horizons at P3 and P4, higher standard deviation values were observed. For the horizon C of P1, a high standard deviation was observed, indicating that the mean is not representative of the behavior observed between repetitions.

The data from the wetting and drying cycles indicate the absence of petroplinthites and the presence of a low volume of resistant material, all visually identified as saprolites associated with slight hardness, easily breakable between the thumb and index finger, with the exception of the P4 Bt sample that it consisted of quartz and chalcedony fragments associated with extreme hardness. The predominant disaggregation of the samples in the wetting and drying cycles can be seen in figures 4 and 5.

For P3 Bt peds, in replicates 3 and 2, in the 2 and 8 h tests, respectively, resistance to disaggregation of 80 and 81 % was observed (Figure 2). It is clear from the image that

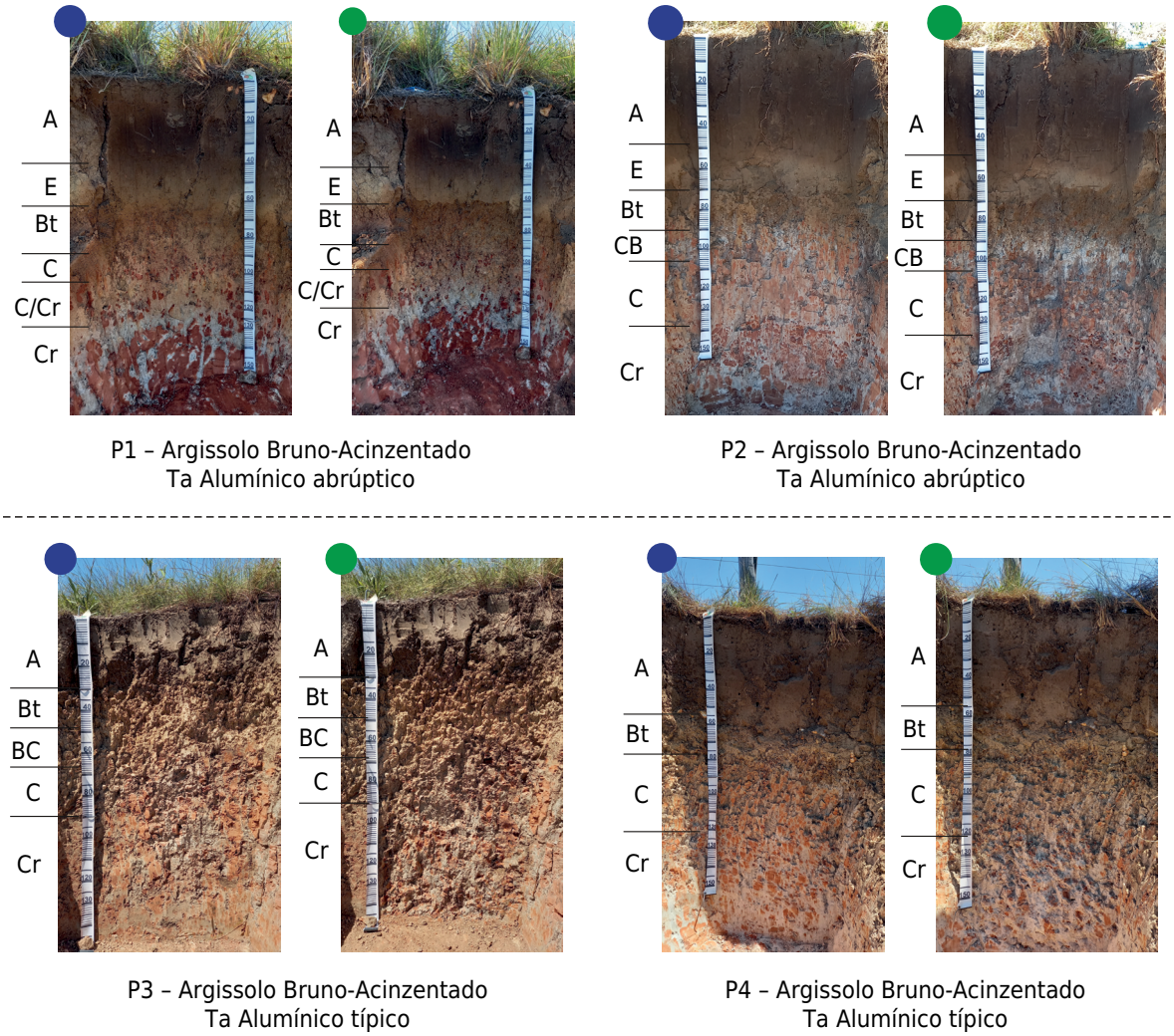

Figure 1. Images of soil profiles with different preparations just scraped with a tile spade (blue circles) and cleaned with a knife – toilet (green circles).

Table 3. Morphological tests for plinthite identification: test of submersion in water for 2 and 8 hours and test of wetting and drying cycles of samples in soils with high textural contrast in southern Brazil

Samples	2 hour test		8 hour test		wetting and drying cycles test		
	% medium resistent	SD	% medium resistent	SD	% medium resistent	Hardness	Sample nature
P1 Bt	1	0.34	3	0.39	0	-	-
P1 C	30	41.11	6	3.97	0	-	-
P1 Cr	1	1.25	1	1.25	2	SH	saprolite
P2 Bt	1	0.10	1	0.66	0	-	-
P2 CB	9	1.81	6	5.00	0	-	-
P2 Cr	5	2.80	2	2.8	0	-	-
P3 Bt	83	2.78	82	1.51	4	SH	saprolite
P3 C	80	0.61	71	11.47	6	SH	saprolite
P3 Cr1	58	16.80	71	9.00	0	-	-
P4 Bt	10	2.14	13	2.7	2	EH	quartz/ chalcedony
P4 C	74	4.82	70	8.57	3	SH	saprolite
P4 Cr	69	18.00	83	4.43	1	SH	Saprolite

SD: standard deviation; SH: slightly hard; EH: extremely hard.

the ped was practically not crumbled in water and also does not show reddish nodules that could suggest the presence of plinthites or saprolite fragments. The same pattern was observed for the resistant fragments of P4 Bt, despite the lower values of 13 and 16 % in the 2 and 8 hours tests, respectively. Replicates 2 of P1 C also makes it clear that the aggregate refers to a fragment of saprolithic material, with a resistance of

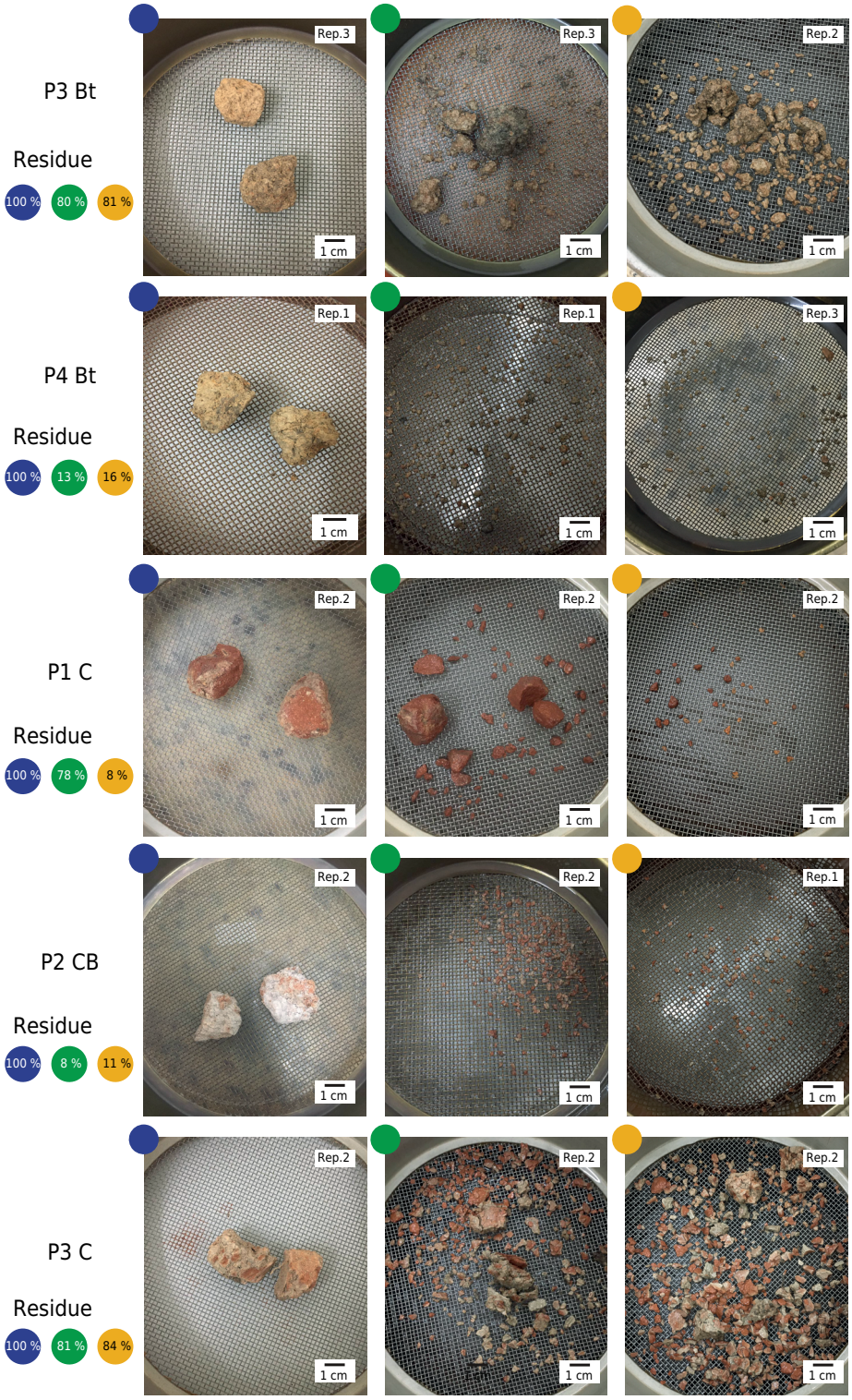

Figure 2. Images selected from the morphological tests for plinthite identification: 2 h water submersion test and 8 h water submersion test. Samples with volume equal to or greater than 5 %. Blue circles: initial samples; green circles: samples after 2 h of submersion in water; orange circles: samples after 8 h of submersion in water.

78 %, similar to replicate 2 of P3 C, fragmented into edged, almost laminar portions, and the Cr samples from P3 and P4 (Figure 3).

After the third cycle of wetting and drying, it is no longer possible to visualize the presence of resistant fragments in the P1 and P2 samples (Figure 4). In the other profiles, small fragments persist even after the fifth cycle, especially in P3 Bt and P4 Cr (Figure 5).

Table 4 shows the granulometric composition of the matrix and mottles present in the analyzed horizons. The high values of the silt/clay ratio indicate the predominance of silt over clay in the samples. In the Bt horizons of the profiles, the highest clay contents

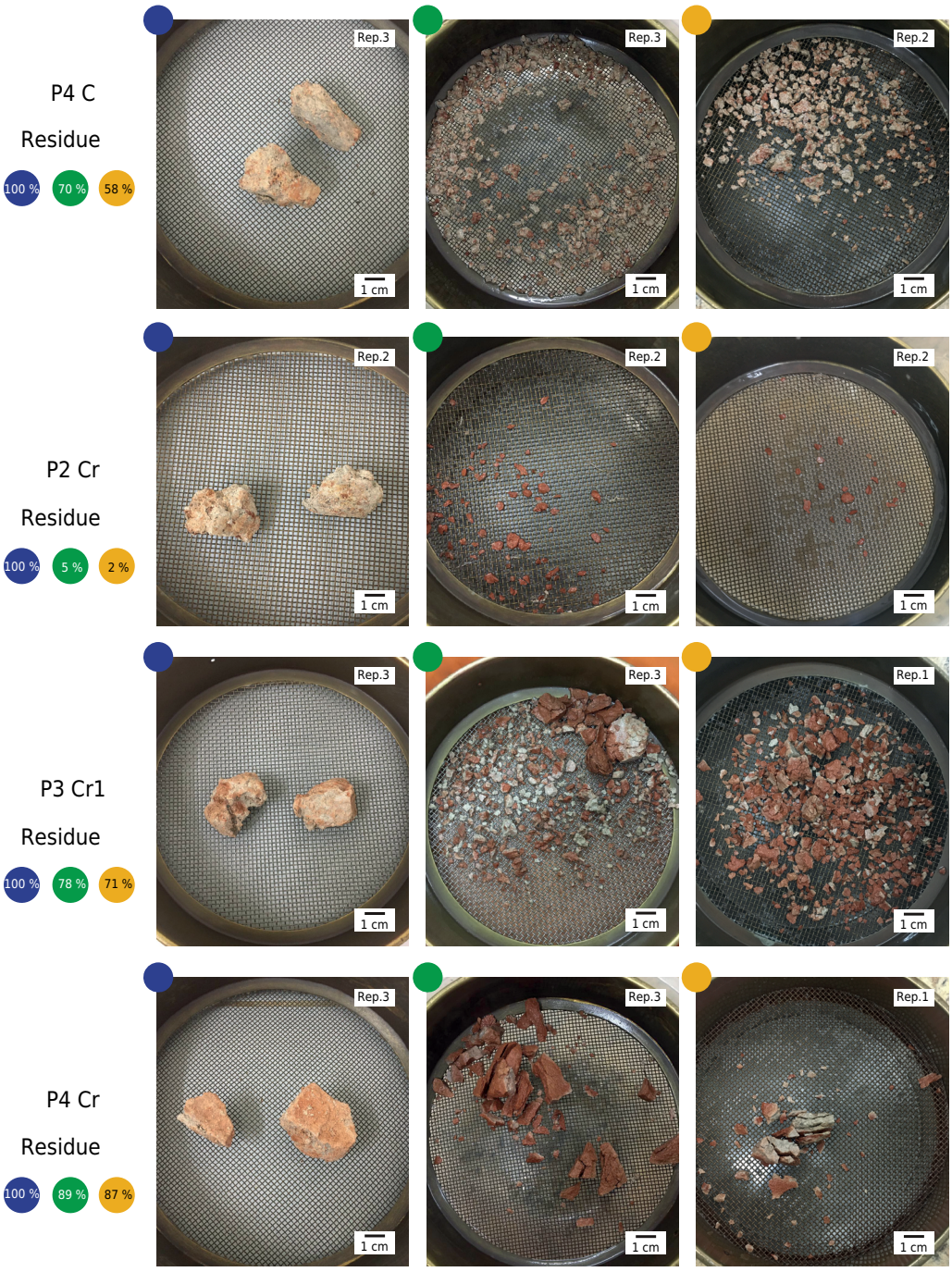

Figure 3. Images selected from the morphological tests for plinthite identification: 2 h water submersion test and 8 h water submersion test. Samples with volume equal to or greater than 5 %. Blue circles: initial samples; green circles: samples after 2 h of submersion in water; orange circles: samples after 8 h of submersion in water.

are verified. The samples presented textural classes ranging from loamy sand – loam – sandy loam – silty loam. There was an increase in the levels of sand at depth. With the exception of the Bt horizons in P2 and P4, for the others, a reduction in clay contents was observed in the mottles compared to the matrix. The sand fraction generally increases in the mottles compared to the matrix. In two-thirds of the analyzed horizons, the mottles presented the same textural class as their corresponding matrix. The source material sample (RCr) of P1 has the sandy texture (loamy sand).

Figure 6 shows the data of sand fractions for the matrix and mottles samples. In general, fractions of larger diameter have a smaller volume, especially in very coarse sand (VCS). For P3 and P4, a similar pattern was observed, with higher contents in the very fine sand (VFS) fraction, except in the Cr horizon of P4, where the highest values correspond to

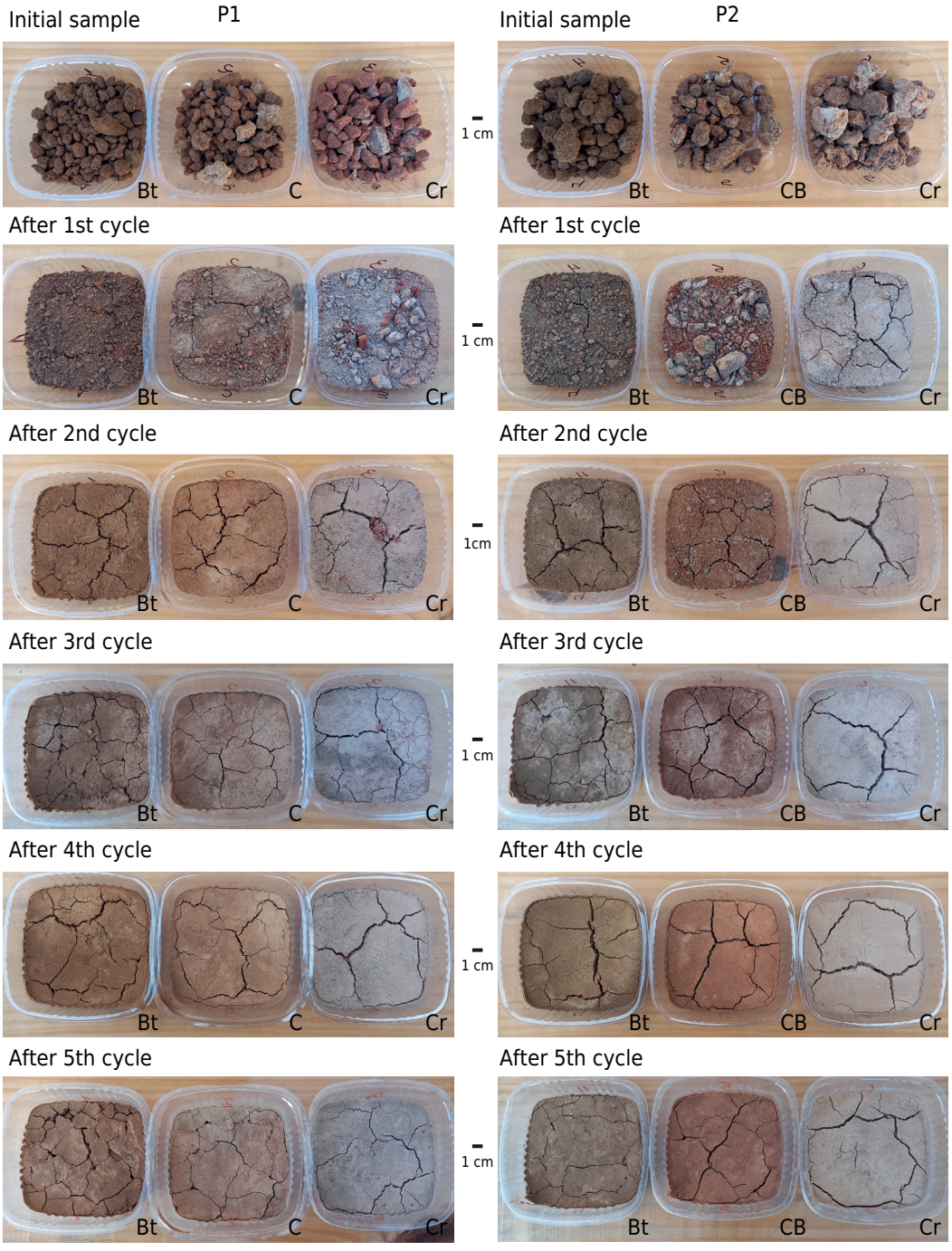

Figure 4. Images of the wetting and drying cycles test to P1 and P2.

fine sand (FS) with 44 % in the matrix and 39 % in mottles. In P1 and P2, the highest percentages are represented in FS, ranging from 28 to 59 %. In this same fraction, it is verified that the values of the matrix samples are a little higher when compared to the mottles in P3 and P4, which is also observed in the VFS fraction of P1. At the Cr horizon of P2, a considerable increase can be seen in the matrix samples compared to the mottles in the FS and VFS fractions.

Table 5 shows the Fe and K data. The iron contents obtained with HCl were lower than those obtained with DCB for the P1 and Bt horizons of P2. For all samples the Fe_{HCl} contents were higher in the mottles. In the extraction with DCB, the Bt horizons showed the highest contents in all profiles, both for the matrix and for the mottles. For the mottles, there were higher contents compared to the matrix, a pattern that was also observed

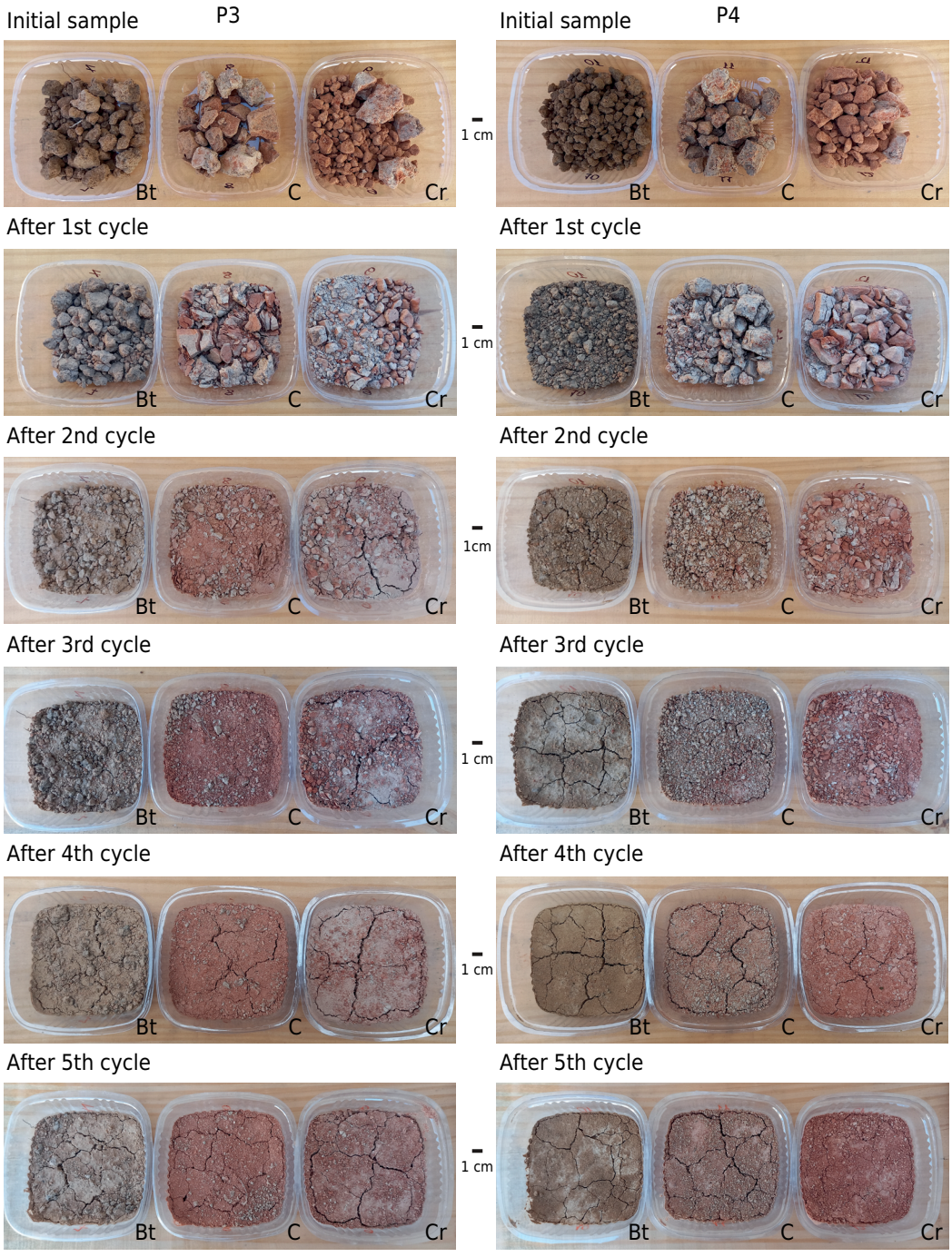

Figure 5. Images of the wetting and drying cycles test to P3 and P4.

Table 4. Coarse fragments, sand, silt and clay contents, silt/clay ratio and texture class of the matrix and mottles samples in soils with high textural contrast in southern Brazil

Samples	Coarse fragments (>2 mm)	Sand	Silt	Clay	silt/clay ratio	Textural class
	g kg^{-1}					
P1 Bt matrix	142	386	419	195	2.1	Loam
P1 Bt mottle		408	413	179	2.3	Loam
P1 C matrix	149	509	364	126	2.9	Loam
P1 C mottle		735	207	58	3.6	Sandy loam
P1 Cr matrix	900	535	344	121	2.8	Sandy loam
P1 Cr mottle		784	184	32	5.6	Loamy sand
P1 RCr	1000	808	177	15	11.8	Loamy sand
P2 Bt matrix	102	439	394	167	2.4	Loam
P2 Bt mottle		382	429	189	2.3	Loam
P2 CB matrix	267	416	430	154	2.8	Loam
P2 CB mottle		432	422	146	2.9	Loam
P2 Cr matrix	750	511	418	71	5,.9	Sandy loam
P2 Cr mottle		405	509	86	5.9	Loam to silt loam
P3 Bt matrix	178	294	571	135	4.2	Silt loam
P3 Bt mottle		304	586	110	5.3	Silt loam
P3 C matrix	171	242	702	56	12.5	Silt loam
P3 C mottle		322	660	19	34.7	Silt loam
P3 Cr1 matrix	710	403	559	38	14.7	Silt loam
P3 Cr1 mottle		499	484	17	28.5	Sandy loam
P3 RCr	1000	524	466	10	46.6	Sandy loam
P4 Bt matrix	188	372	455	174	2.6	Loam
P4 Bt mottle		331	472	197	2.4	Loam
P4 C matrix	160	284	576	140	4.1	Silt loam
P4 C mottle		534	443	23	19.3	Sandy loam
P5 Cr matrix	680	553	398	49	8.1	Sandy loam
P4 Cr mottle		677	309	14	22.1	Sandy loam

for the extraction with OAA. In all extractions, Fe contents decreased with depth. The highest values of Fe were determined in the DCB, ranging from 20 to 50 g kg^{-1}, in the mottles samples. The Fe_{OAA} contents were lower than 1 g kg^{-1} for all samples, resulting in low values of the Fe_{OAA}/Fe_{DCB} ratio.

In the extraction of $K_{Mehlich\text{-}1}$, the highest contents were observed in the samples of the matrix, with the exception of the horizon C and Cr of P1 and Cr of P2, in which there is a considerable increase in the K content in the mottles. The contents extracted with HNO_3 were higher in relation to $K_{Mehlich\ 1}$, reaching the value of 1691.40 mg L^{-1} (P3 C matrix). In P1 and P2, the matrix samples showed higher values when compared to the mottles, except for Cr. In the P3 and P4 profiles, an inverse pattern was observed, with the exception of the P3 C horizon. In both extractions, the most expressive K contents are concentrated in the C and Cr horizons.

Profiles P1 and P2 presented identical diffraction patterns, as well as P3 and P4. The mineralogy of the clay fraction (Figure 7) indicates the predominance of 2:1 minerals, smectite (reflections 18.84 – 12.81 – 1.00 Å) followed by mica (illite) seen in reflections 1.00 – 4.97 Å) and kaolinite (reflections 7.15 – 3.58 Å). The presence of interstratified

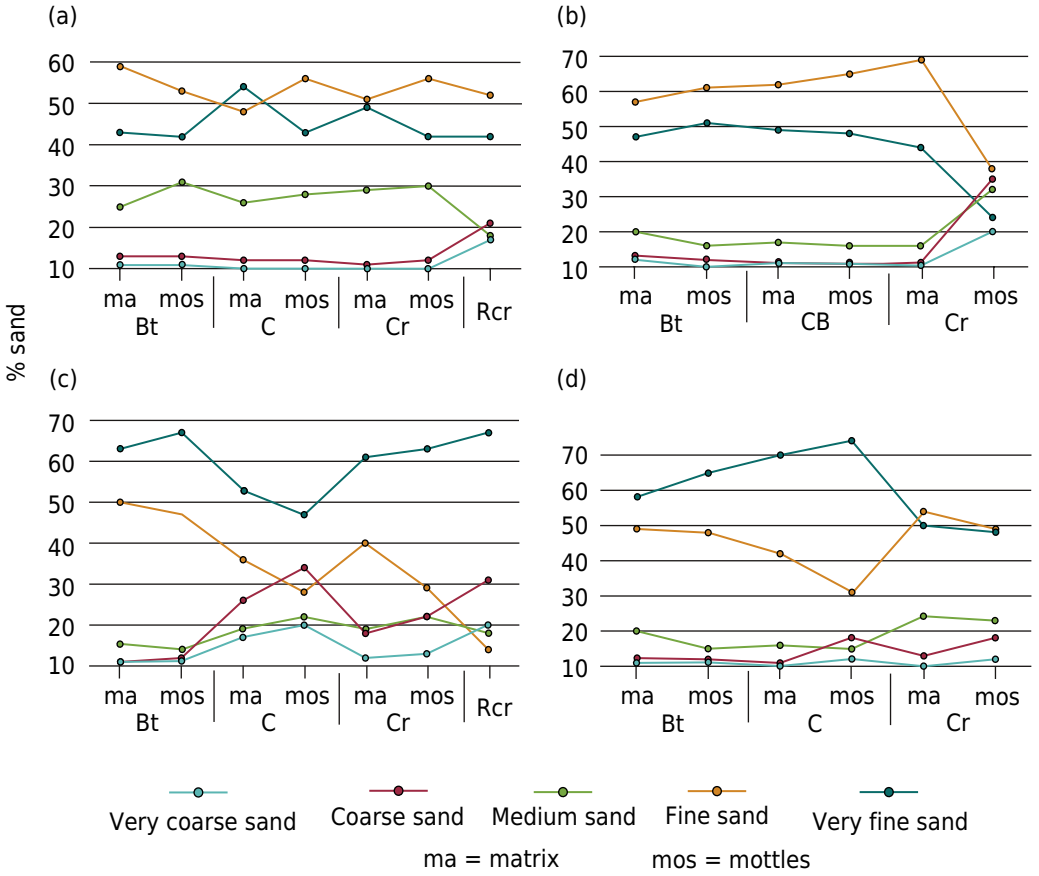

Figure 6. Sand fractions of the matrix and mottles samples in soils with high textural contrast in southern Brazil. a: P1; b: P2; c: P3; and d: P4.

illite-smectite and illite-kaolinite is also evident in the shoulders formed around the 1.00 Å reflection, both for larger and smaller 2θ angles. Kaolinite-illite is also seen in the shoulder between 3.58–3.34 Å. The presence of quartz was identified by the 4.26 – 3.34 Å reflexes. The residue of plagioclase, possibly microcline, is suggested by reflections 3.24 – 3.19 Å in the mottles sample from the Cr horizon of P4. The partial contraction of the layers 2:1 in the treatment with K heated to 300 °C indicates the presence of smectite with hydroxy-Al interlayers, expressive in P3 and P4.

The rock samples showed the same diffraction pattern (Figure 7c). The samples presented a predominance of quartz (reflections 4.26 - 3.35 - 2.46 - 2.23 - 2.13 - 1.82 - 1.54 Å) followed by mica (reflections 4.50 - 3.88 - 3.66 – 2.93 – 2.57 – 1.98 – 1.67 – 1.45 Å) and potassium and alkali feldspars (reflections 3.78 – 3.26 – 3.20 – 3.03 Å).

There was no mineralogical difference between the matrix and mottles samples for the same horizon. However, in P1 and P2, the Cr horizon presents a greater expression of illite in relation to kaolinite when compared to the more superficial horizons. In P3 and P4, in the C and Cr horizons, the greater alteration of plagioclase in the matrix is visible in relation to the mottles.

DISCUSSION

It is important to highlight that the different preparations of the soil profiles for description (Figure 1) influence the estimation of mottles. Except for the Bt horizon of P1, the percentages presented after knife cleaning (toilet) are lower compared to the scraped face (Table 2). This happens because, in this case, the Fe reduction process predominates in the external portion of the peds (Aide et al., 2004), where the humidity

Table 5. Selective chemical dissolution data of Fe and K in soils with high textural contrast in southern Brazil.

Sample	Fe_{HCl}	Fe_{DCB}	Fe_{OAA}	Fe_{DCB}/Fe_{HCl}	Fe_{OAA}/Fe_{DCB}	$K_{Mehlich\ I}$	K_{HNO3}
	g kg^{-1}					mg L^{-1}	
P1 Bt matrix	7.89	10.80	0.32	1.37	0.03	11.69	471.67
P1 Bt mottle	32.38	35.52	0.46	1.10	0.01	10.67	461.38
P1 C matrix	7.60	10.30	0.22	1.36	0.02	14.16	450.00
P1 C mottle	13.31	32.39	0.41	2.43	0.01	19.14	435.64
P1 Cr matrix	3.17	1.41	0.01	0.44	0.01	29.55	530.96
P1 Cr mottle	10.56	12.45	0.16	1.18	0.01	46.63	537.50
P1 RCr	10.50	7.00	0.07	0.67	0.01	15.66	633.25
P2 Bt matrix	6.90	9.11	0.26	1.32	0.03	29.67	455.74
P2 Bt mottle	35.27	51.20	2.07	1.45	0.04	20.69	299.25
P2 CB matrix	5.79	5.04	0.20	0.87	0.04	29.13	467.78
P2 CB mottle	18.76	17.57	0.72	0.94	0.04	27.67	390.33
P2 Cr matrix	4.21	2.81	0.07	0.67	0.02	34.60	498.69
P2 Cr mottle	36.08	28.86	0.55	0.80	0.02	55.14	1523.04
P3 Bt matrix	10.76	4.30	0.17	0.40	0.04	26.17	636.07
P3 Bt mottle	24.28	23.86	0.63	0.98	0.03	nd	647.90
P3 C matrix	6.38	1.39	0.01	0.22	0.00	66.60	1691.40
P3 C mottle	12.70	10.10	0.22	0.80	0.02	56.64	1351.86
P3 Cr1 matrix	5.27	1.12	0.01	0.21	0.00	41.12	967.61
P3 Cr1 mottle	11.94	7.90	0.13	0.66	0.02	30.66	1069.66
P3 RCr	6.50	4.42	0.01	0.68	0.00	10.69	819.04
P4 Bt matrix	9.46	5.73	0.34	0.61	0.06	26.14	470.43
P4 Bt mottle	24.97	20.40	0.34	0.82	0.02	20.15	525.62
P4 C matrix	4.47	2.56	0.05	0.57	0.02	22.66	599.32
P4 C mottle	14.42	14.25	0.40	0.99	0.03	11.68	804.46
P4 Cr matrix	2.47	0.69	0.03	0.28	0.04	13.19	500.74
P4 Cr mottle	9.81	5.64	0.12	0.58	0.02	10.69	632.99

nd: not determined.

is higher, while the internal portion remains in an oxidation state, with a reddish color. The blade cut shows, in a more expressive way, the mottles referring to the internal portions of the peds.

The wet consistency of plinthites varies from firm to very firm (Daniels et al., 1978). However, it appears that many of the mottles samples had a friable consistency (Table 2), contributing to the fact that these features were not considered plinthites in the field. The abundant presence of mica in these materials was also observed, suggesting their saprolithic nature, since the sediment of the Sanga do Cabral formation has a large amount of this mineral (Sartori, 2009).

The occurrence of petroplinthite was not observed in the evaluated profiles, as suggested by Almeida and Santos (2021) to support the presence of plinthites. This fact provides further evidence that the reddish features present in these soils are not plinthic materials or are in an incipient process to be identified as plinthites.

Generally, plinthites are red or dark red, with hues ranging from 10 R to 7.5 YR (IBGE, 2015; Santos et al., 2018). However, this coloration is also verified in the

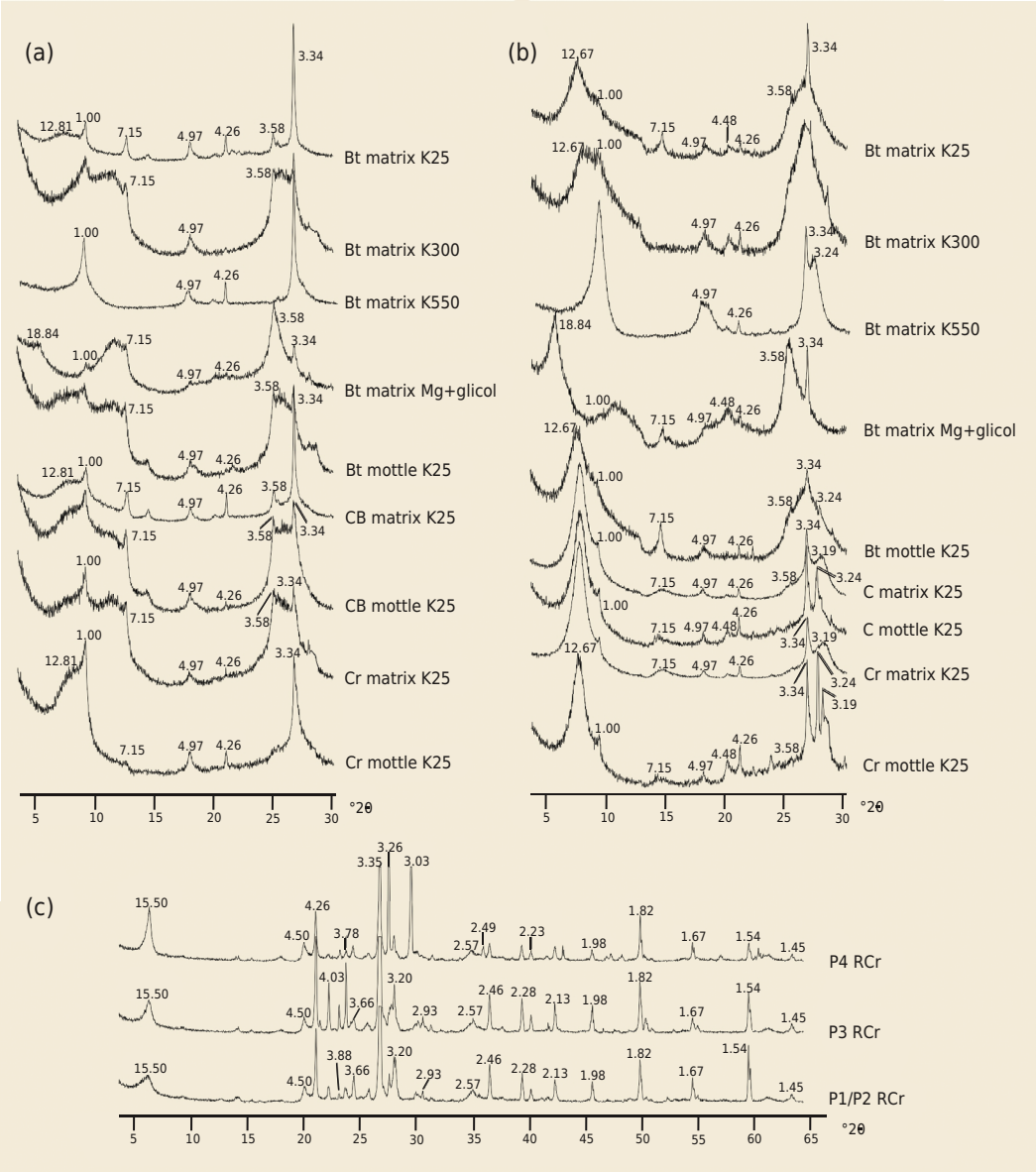

Figure 7. X-ray diffractograms of the clay fraction of the matrix and mottles samples from profile 2 (a) and profile 4 (b) and from rock samples (c). Values of "d" (interplanar distance) in Angstrom (Å).

saprolite, making it difficult to separate these materials. In the mottles, the colors between hues 10 R and 5 YR (Table 2) did not prove to be an effective variable for such distinction.

The 2 and 8 h water submersion tests indicated, respectively, by Wood and Perkins (1976) and Daniels et al. (1978), and recommended by Anjos et al. (1995) and Batista and Santos (1995) for the identification of plinthites were not efficient to differentiate plinthite from saprolite. This is because the tests suggest the material resistant after certain periods of submersion should be identified as plinthite. However, the material that resisted in high percentages in all horizons of P3 and in the C and Cr of P4 maintains the typical structure of sedimentary saprolite (Figures 2 and 3) showing laminar ruptures when drying. In P1 and P2, despite most of the peds not having resisted, it is possible to affirm based on the morphology that the P1 C material is also saprolite, observing the permanence of the peds in the 2 h test (Figure 2). Furthermore, a sample of ped from P3 Bt without mottles resisted to the water disaggregation test, indicating that even soil peds can resist the test.

The percentages of resistant material do not show significant variations between the two tests (Table 3). Considering the time of performance, the Wood and Perkins test (1976) can be indicated as an adequate alternative, especially when performed in the field; however, its use requires attention due to the resistance also manifested by the saprolite. Also, the weathering degree of saprolites in this study does not affect the results of water submersion tests, once the different weathering classes present in the Bt, CB, C and Cr horizons presented similar behavior. Therefore, further studies are needed to develop a safe morphological test, especially in the field, which guarantees the correct identification of these features.

The wetting and drying cycles test indicated the absence of petroplinthites that should have been formed from the irreversible hardening of the plinthites (Jacomine et al., 2010; Eze et al., 2014). The presence of a low volume of resistant material, with light hardness, easily breakable between the fingers, indicated that the cycle test, despite being laborious, was efficient in the perception of the saprolite.

In general, there was a reduction in clay contents and an increase in the sand and silt fractions in the mottles (Table 4), corroborating the values found for plinthites in previously published studies (Wood and Perkins, 1976; Anjos et al., 1995) and expected for sandy saprolithic materials in southern Brazil. Even so, no major changes were observed in the texture of the evaluated horizons, so many of them remained in the same textural class. Therefore, the granulometry was also inefficient in confirming plinthite or saprolite's presence.

Despite the low clay contents in the evaluated samples, the high levels of silt and sand, especially fine and very fine sand, contribute to the lower porosity of the subsurface horizons. According to data from Pedron et al. (2015) for the same profiles of Alisols, the macroporosity varies from 0.14 in Bt to 0.07 m^3 m^{-3} in Cr and the density from 1.4 in Bt to 1.7 kg dm^{-3} in Cr, contributing for the reduction of permeability, elevation of humidity and formation of the presented redoximorphic features.

The Fe contents (Fe_{HCl}) are relatively low for all the profiles. The Fe_{OAA}/Fe_{DCB} ratios were extremely low, evidencing the predominance of crystalline forms of Fe. As expected, the Fe contents in mottles are higher than those in matrix (Daniels et al.,1978; Anjos et al., 1995; Miguel et al., 2013; Almeida and Santos, 2021). Nevertheless, according to Almeida and Santos (2021), when the Fe data were related to the morphological test of the soil wetting and drying cycles, the authors found that the increases in Fe contents in the mottles were not sufficient to confirm its plinthic nature. The material's resistance to disaggregation in water presented in table 2 also shows that there is no relationship with the increases in Fe contents in the mottles, especially for P1 and P2. Furthermore, in profiles P3 and P4, the high values of resistance to disaggregation are associated either with the soil (P3 Bt) or with the domain of saprolithic material (C and Cr of P3 and P4).

Iron segregation from the matrix and its concentration in the mottles occurs due to the oxide reduction process promoted by excess moisture (Eze et al., 2014). This process results in a decrease in the levels of this element in the matrix, which presents grayish colors, characterizing a depletion zone (Costantini and Priori, 2007). In the peds, an oxic environment is observed inside, allowing the re-oxidation or even the maintenance of crystalline Fe oxides present in the material, characterizing the mottles (Aide et al., 2004).

The high values of non-exchangeable K (K_{HNO3}) corroborate the abundance of mica in the parent material (Sartori, 2009) and stand for a high mineral reserve of this element in the studied soils. An increase in K contents was also observed at depth, which was expected due to the lower weathering in the underlying horizons. The expectation of higher levels of non-exchangeable K in the mottles, suggesting its saprolithic nature, was confirmed for most of the profiles and horizons evaluated. For the RCr layer of

P1, a higher content of non-exchangeable K is observed compared to the other soil layers, while the opposite occurs in P3, with the highest values expressed in the C and Cr horizons. This fact may be the result of the stratified occurrence of mica in the sediments of the Sanga do Cabral formation, as well as the clay balls and carbonate concretions also present.

The clay fraction mineralogy indicated similarity between all the profiles, where P1 and P2 differ from P3 and P4 only by the weathering degree of the minerals. The greater preservation of plagioclase in the mottle samples at C and Cr of profiles 3 and 4 indicates the saprolithic nature of the material. Likewise, the expressive presence of interstratified illite-smectite and illite-kaolinite, mainly in profiles 1 and 2, associated with the predominance of 2:1 minerals, indicate a lower pedogenetic development of the soil horizons, their high clay activity, associated with the argilluviation-ferrolysis processes, without the presence of plinthization, as also observed by Almeida and Santos (2021) in some profiles of this region. The high aluminum contents observed by Pedron et al. (2015) in these profiles are the result of the alteration of the smectites with hydroxy-Al interlayers resulting from the ferrolysis process (Almeida and Santos, 2021).

CONCLUSIONS

The saprolite proved to be resistant in the tests of submersion in water (disaggregation in water), making it difficult to interpret the results for the correct identification between plinthites and saprolite fragments. The test of the wetting and drying cycles allowed the identification of the saprolite, since there was no significant hardening of the resistant material. The morphological field data associated with the results of the test of the wetting and drying cycles, with the K dissolution and mineralogy data, indicate the saprolithic nature of the mottles in all horizons and profiles.

AUTHOR CONTRIBUTIONS

Conceptualization: Fabrício de Araújo Pedron (lead).

Data curation: Fabrício de Araújo Pedron (equal) and Mariana Rigueira da Costa Pereira (equal).

Formal analysis: Fabrício de Araújo Pedron (equal), José Eduardo Dias Alves (equal) and Mariana Rigueira da Costa Pereira (equal).

Investigation: Fabrício de Araújo Pedron (equal) and Mariana Rigueira da Costa Pereira (equal).

Methodology: Fabrício de Araújo Pedron (equal) and Mariana Rigueira da Costa Pereira (equal).

Project administration: Fabrício de Araújo Pedron (lead).

Writing – original draft: Fabrício de Araújo Pedron (equal) and Mariana Rigueira da Costa Pereira (equal).

Writing – review & editing: Fabrício de Araújo Pedron (equal), José Eduardo Dias Alves (equal), Mariana Rigueira da Costa Pereira (equal), Ricardo Bergamo Schenato (equal) and Ricardo Simão Diniz Dalmolin (equal).

REFERENCES

Aide M, Pavich Z, Lilly ME, Thornton R, Kingery W. Plinthite formation in the coastal plain region of Mississippi. Soil Sci. 2004;169:613-23. https://doi.org/10.1097/01.ss.0000142636.77482.e0

Almeida JA, Santos PG. Epi and endosaturation affecting redoximorphic features and pedogenesis in subtropical soils with high textural contrast developed from sedimentary rocks. Rev Bras Cienc Solo. 2021;45:e0210044. https://doi.org/10.36783/18069657rbcs20210044

Anjos LHC, Franzmeier DP, Schulze DG. Formation of soils with plinthite on a toposequence in Maranhão State, Brazil. Geoderma. 1995;64:257-79. https://doi.org/10.1016/0016-7061(94)00022-3

Anjos LHC, Pereira MG, Perez DV, Ramos DP. Caracterização e classificação de Plintossolos no município de Pinheiro – MA. Rev Bras Cienc Solo. 2007;31:1035-44. https://doi.org/10.1590/S0100-06832007000500020

Batista MA, Santos MC. Morfologia e gênese de dois solos com plintita da região Meio- Norte do Brasil. Rev Bras Cienc Solo. 1995;19:287-96.

Brindley GW, Brown G. Crystal structures of clay minerals and their X-ray identification. London: Mineralogical Society; 1980.

Costantini EAC, Priori S. Pedogenesis of plinthite during early Pliocene in the Mediterranean environment: Case study of a buried paleosol at Podere Renieri, Central Italy. Catena. 2007;71:425-43. https://doi.org/10.1016/j.catena.2007.03.015

Daniels RB, Perkins HF, Hajek BF, Gamble EE. Morphology of discontinuous phase plinthite and criteria for its field identification in the southeastern United States. Soil Sci Soc Am J. 1978;42:944-9. https://doi.org/10.2136/sssaj1978.03615995004200060024x

Dick DP, Kämpf N. Comparação da extração de ferro com HCl 6N, H_2SO_4 1:1 e ditionito-citrato-bicarbonato de sódio em horizontes B-latossólicos. Rev Bras Cienc Solo. 1988;12:185-8.

Eze PN, Udeigwe TK, Meadows ME. Plinthite and its associated evolutionary forms in soils and landscapes: a review. Pedosphere. 2014;24:153-66. https://doi.org/10.1016/S1002-0160(14)60002-3

Gubiani PI, Almeida TA, Mulazzani RP, Pedron FA, Suzuki LEAS, Pereira CA. Shaking settings to reduce the breakdown of Entisol fragile particles in texture analysis. Rev Bras Cienc Solo. 2021;45:e0210066. https://doi.org/10.36783/18069657rbcs20210066

Hughes RE, Moore DM, Glass HD. Qualitative and quantitative analysis of clay minerals in soils. In: Amonette JE, Zelazny LW, editors. Quantitative methods in soil mineralogy. Madison: Soil Science Society of America; 1994. p. 330-59.

Instituto Brasileiro de Geografia e Estatística - IBGE. Manual técnico de pedologia. 3. ed. Rio de Janeiro: IBGE; 2015.

IUSS Working Group WRB. World reference base for soil resources 2014, update 2015: International soil classification system for naming soils and creating legends for soil maps. Rome: Food and Agriculture Organization of the United Nations; 2015. (World Soil Resources Reports, 106).

Jackson ML. Soil chemical analysis: Advanced course. 2nd ed. Madison: University of Wisconsin; 1985.

Jackson ML, Lim CH, Zelazny LW. Oxides, hydroxides, and aluminosilicates In: Klute A, editor. Methods of soil analysis - Part 1: Physical and mineralogical methods analysis. 1st ed. Madison: American Society of Agronomy; 1986. p. 101-150. https://doi.org/10.2136/sssabookser5.1.2ed.c6

Jacomine PKT, Araujo Filho JC, Lima JFWF. Testes para identificação de plintita em solos da formação Solimões no Acre. In: Anais da 9ª Reunião Brasileira de Classificação e Correlação de Solos - Solos sedimentares em sistemas amazônicos: potencialidades e demandas de pesquisa; 2010. Rio Branco, AC. Rio Branco, AC: SBCS; 2010. p. 27-32.

Juilleret J, Azevedo AC, Santos RA, Santos JCB, Pedron FA, Dondeyne S. Where are we with whole regolith pedology? A comparative study from Brazil. South Afr J Plant Soil. 2018;35:251-61. https://doi.org/10.1080/02571862.2017.1411537

Karathanasis AD, Hajek BF. Revised methods for rapid quantitative determination of minerals in soil clay. Soil Sci Soc Am J. 1982;46:419-25. https://doi.org/10.2136/sssaj1982.03615995004600020042x

Knudsen D, Peterson GA, Pratt PF. Lithium, sodium and potassium. In: Page AL, editor. Methods of soil analysis: Part 2 - Chemical and microbiological properties. 2nd ed. Madison: American Society of Agronomy; 1983. p. 225-46. https://doi.org/10.2134/agronmonogr9.2.2ed.c13

Maluf JRT. Nova classificação climática do Estado do Rio Grande do Sul. Rev Bras Agrometeorol. 2000;8:141-50.

Martins APB, Santos GG, Oliveira VA, Maranhão DDC, Collier LS. Hardening and stability of plinthic materials of the Araguaia River floodplain under different drying treatments. Rev Bras Cienc Solo. 2018;42:170-90. https://doi.org/10.1590/18069657rbcs20170190

Martins R, Melo VF, Serrat BM. Reserva mineral de potássio em solos dos campos gerais, estado do Paraná. Rev Ceres. 2004;51:521-33.

McKeague JA, Day JH. Dithionite- and oxalate-extractable Fe and Al as aids in differentiating various classes of soil. Can J Soil Sci. 1966;46:13-22. https://doi.org/10.4141/cjss66-003

Mehra OP, Jackson ML. Iron oxide removal from soils and clays by a dithionite-citrate system buffered with sodium bicarbonate. Clays Clay Miner. 1960;7:317-27. https://doi.org/10.1016/B978-0-08-009235-5.50026-7

Miguel P, Dalmolin RSD, Pedron FA, Fink JR, Moura-Bueno JM. Caracterização de plintitas e petroplintitas em solos da Depressão Central do Rio Grande do Sul. Cienc Rural. 2013;43:999-1005. https://doi.org/10.1590/S0103-84782013005000065

Pedron FA, Azevedo AC, Dalmolin RSD, Stürmer SLK, Menezes FP. Morfologia e classificação taxonômica de Neossolos e saprolitos derivados de rochas vulcânicas da formação Serra Geral no Rio Grande do Sul. Rev Bras Cienc Solo. 2009;33:119-28. https://doi.org/10.1590/S0100-06832009000100013

Pedron FA, Dalmolin RSD. Solos arenosos do Bioma Pampa brasileiro. Santa Maria: Editora UFSM; 2019.

Pedron FA, Fink JR, Dalmolin RSD, Azevedo AC. Morfologia dos contatos entre solo-saprolito-rocha em Neossolos derivados de arenitos da Formação Caturrita no Rio Grande do Sul. Rev Bras Cienc Solo. 2010;34:1941-50. https://doi.org/10.1590/S0100-06832010000600019

Pedron FA, Oliveira RB, Dalmolin RSD, Azevedo AC, Kilca RV. Boundary between Soil and Saprolite in Alisols in the South of Brazil. Rev Bras Cienc Solo. 2015;39:643-53. https://doi.org/10.1590/01000683rbcs20140229

Pedron FA, Samuel-Rosa A, Dalmolin RSD. Variation in pedological characteristics and the taxonomic classification of Argissolos (Ultisols and Alfisols) derived from sedimentary rocks. Rev Bras Cienc Solo. 2012;36:1-9. https://doi.org/10.1590/S0100-06832012000100001

Resende M, Curi N, Ker JC, Rezende SB. Mineralogia de solos brasileiros: Interpretações e aplicações. Lavras, MG: UFLA; 2005.

Santos HG, Jacomine PKT, Anjos LHC, Oliveira VA, Lumbreras JF, Coelho MR, Almeida JA, Araújo Filho JC, Oliveira JB, Cunha TJF. Sistema brasileiro de classificação de solos. 5. ed. rev. ampl. Brasília, DF: Embrapa; 2018.

Santos RD, Lemos RC, Santos HG, Ker JC, Anjos LHC, Shimizu SH. Manual de descrição e coleta de solo no campo. 7. ed. rev. e ampl. Viçosa, MG: Sociedade Brasileira de Ciência do Solo; 2015.

Sartori PLP. Geologia e geomorfologia de Santa Maria. Cienc Amb. 2009;38:19-42.

Schoeneberger PJ, Wysocki DA, Benham EC. Field book for describing and sampling soils. Version 3.0. Lincoln, NE: National Soil Survey Center; Natural Resources Conservation Service, U.S. Department of Agriculture; 2012.

Teixeira PC, Donagemma GK, Fontana A, Teixeira WG. Manual de métodos de análise de solo. 3. ed. rev e ampl. Brasília, DF: Embrapa; 2017.

Whitting LD, Allardice WR. X-ray diffraction techniques. In: Klute A, editor. Methods of soil analysis: Part 1 - Physical and mineralogical methods. 2nd ed. Madison: American Society of Agronomy; 1986. p. 331-62. https://doi.org/10.2136/sssabookser5.1.2ed.c12

Wood BW, Perkins HF. Plinthite characterization in selected southern coastal plain soils. Soil Sci Soc Am J. 1976;40:143-6. https://doi.org/10.2136/sssaj1976.03615995004000010038x